

1 Applicability of Synthetic Aperture Radar (SAR) to Evaluate Leaf Area Index (LAI) and  
2 its Growth Rate of Rice in Farmers' Fields in Lao PDR

3 Yoshihiro HIROOKA<sup>a, b</sup>, Koki HOMMA<sup>\*a</sup>, Masayasu MAKI<sup>c</sup>, Kosuke SEKIGUCHI<sup>c</sup>

4 <sup>a</sup>Graduate School of Agriculture, Kyoto University, Kyoto 606-8502, Japan

5 <sup>b</sup>Research Fellow of Japan Society for the Promotion of Science

6 <sup>c</sup>Graduate School of Engineering, Kyoto University, Kyoto 615-8530, Japan

7 \* Corresponding author at: Kyoto University, Graduate School of Agriculture,  
8 Kitashirakwa-Oiwake, Sakyo, Kyoto 606-8502, Japan. Tel.: +8175 753 6042; fax: +81  
9 75 753 6065. E-mail address: homma@kais.kyoto-u.ac.jp (K. Homma)

10  
11 Highlights

- 12 • This study applied SAR to estimate LAI and its growth rate in Lao PDR.
- 13 • Back scattering coefficient (BSC) of SAR was correlated with LAI and NDVI.
- 14 • Increase of BSC against day represented LAI growth.

15  
16 ABSTRACT

17 Rice is the most important crop in Lao People's Democratic Republic (Lao PDR).  
18 Synthetic aperture radar (SAR) is proposed as a more suitable method to evaluate rice  
19 growth in this area because it is independent from cloud and solar illumination. This  
20 study analyzed the relationship between the back scattering coefficient (BSC) in SAR  
21 images and leaf area index (LAI) of rice. Here, we discuss the applicability of SAR to  
22 estimate LAI and its growth rate in farmers' fields in Lao PDR. 30 farmers' paddy fields  
23 were selected for surveying throughout the growth period in the wet season of 2013, and  
24 both LAI and normalized difference vegetation index (NDVI) were measured at 4 time  
25 periods before the heading period for each field. X-band SAR images from the  
26 COSMO-SkyMed system (SAR) were used in this study. BSC was significantly  
27 correlated with LAI and NDVI. BSC at 28 of 30 fields was positively correlated with  
28 days after transplanting (DAT), and 10 of these results were significant. The increased  
29 rate in BSC obtained at the fields where BSC and DAT had a significant correlation,  
30 were significantly correlated with that in LAI. This finding suggests that if SAR images  
31 demonstrate significant increases of BSC against DAT, the increased rate may also  
32 represent LAI growth rate, although uncontrollable water levels and weeds occasionally  
33 interrupt observation. This study demonstrates the capacity of SAR to evaluate rice  
34 production in developing countries.

35  
36 Keywords:

37 Back scattering coefficient (BSC); farmers' fields; LAI; NDVI; rice; Synthetic aperture  
38 radar (SAR).

39

## 40 **1. Introduction**

41 Rice is undoubtedly the most important crop in the Lao People's Democratic Republic  
42 (Lao PDR), and approximately 70% of the total calories in the Lao diet come from rice  
43 (Maclean et al., 2002). While improving its productivity is strongly recommended, the  
44 information about rice growth characteristics in farmers' fields is limited (Bell and Seng,  
45 2003; Fukai et al., 1999; Inamura et al., 2003). Hirooka et al. (2015) measured leaf area  
46 index (LAI) and its growth rate using a plant canopy analyzer and reported that rice  
47 production was closely associated with LAI growth rate. However, because application  
48 of a plant canopy analyzer is not suitable on a regional scale, the evaluation by satellite  
49 based remote sensing is recommended.

50 Most rice production in Lao PDR is conducted in the rainy season (Schiller, 2006),  
51 during which cloudy conditions often interrupt satellite observation in visible and near-  
52 infrared range. Accordingly, remote sensing based on synthetic aperture radar (SAR) is  
53 proposed as a more suitable method to evaluate rice growth in this area because the  
54 observation is independent from cloud and solar illumination (Chakraborty et al., 1997).  
55 The radar transmits a pulse and then measures the time delay and strength of the  
56 reflected echo, where the ratio of scattered and incident microwave energy is termed the  
57 back scattering coefficient (BSC) (Moran et al., 2002). SAR uses polarized radiation  
58 and, therefore, can exploit polarization signatures of the imaged scatters for obtaining  
59 more information about the scatter's structure (Bamler, 2000). Although previous  
60 studies investigated the applicability of SAR to estimate LAI (Inoue et al., 2014; Maki  
61 et al., 2015), the estimation accuracy has not attained practical level. The present study  
62 analyzed the relationship between SAR images and LAI of rice measured by Hirooka et  
63 al. (2015) and discusses the applicability of SAR to estimate LAI and its growth rate in  
64 farmers' fields in Lao PDR. The results showed although the accuracy was still the  
65 problems to estimate LAI, analyzing a sequence of BSC may provide a strategy to  
66 applicate SAR to evaluate rice production in developing countries.

67

## 68 **2. Materials and Methods**

### 69 2.1. Overview and test sites

70 This study used LAI data from farmers' fields in Vientiane province in 2013, Lao PDR  
71 (18°01' - 18°30'N, 102°24' - 103°02'E, 168 - 178 m asl.), observed by Hirooka et al.  
72 (2015). We analyzed SAR data in relation to LAI, together with the normalized

73 difference vegetation index (NDVI) measured in the same fields.

74 30 farmers' paddy fields in this area were selected for surveying throughout the growth  
75 period (Hirooka et al., 2015). We selected the fields that had open space in the direction  
76 of satellite orbit (west and approximately 45° in the incident angle) and that were  
77 surrounded by relatively flat paddy fields (at least 1 ha in the area). The mean air  
78 temperature for the measuring period (from 22 July to 16 September) was 28.0 °C. The  
79 longitude and latitude of the selected fields were recorded by Global Positioning System  
80 (GPSMAP 62SJ, Garmin International, Inc., Kansas City). The cultivation methods  
81 (direct seeding/transplanting, fertilizer, planting density and cultivar) of rice plants and  
82 field conditions (standing water and weeds) in the farmers' fields under investigation  
83 were checked by the authors' observation and interviews to farmers. The fields where  
84 the maximum depth of standing water exceeded more than 30 cm were classified as  
85 deep water fields, and the fields where weeds covered a maximum of 20% or more were  
86 classified as weedy fields in this study.

## 87 2.2. LAI measurement and analysis (Hirooka et al., 2015)

88 LAI was measured using a plant canopy analyzer (LAI-2200, LI-COR, Inc., Nebraska)  
89 with a single sensor mode in a sequence of two above and four below canopy with 5  
90 replications at each field. To reduce the influence of the adjacent fields and the operator,  
91 a 90° view-cap was applied to the optical sensor. Measurements were conducted 4 times  
92 before the heading period (22 - 24 July, 10 - 12 August, 30 August - 1 September and 16  
93 - 18 September). Since LAI linearly increased during the measurement, LAI growth rate  
94 was calculated using the following linear function (Eq (1); Hirooka et al., 2015).

$$95 \text{ LAI} = a * \text{DAT} + b \quad (1)$$

96 DAT denotes days after transplanting, a represents LAI growth rate, and b represents  
97 approximate LAI at the transplanting date.

## 98 2.3. NDVI measurement

99 For measuring spectral reflectance of rice canopies, we used a spectroradiometer  
100 (MS-720, EKO Instruments Co., Ltd., Tokyo). MS-720 measures radiation from 350 nm  
101 to 1050 nm by 3.3 nm intervals. We measured the sky radiation with a FOV 180°  
102 attachment and the plant reflection with a FOV 45° attachment from 1 m above the rice  
103 canopies, with 3 replications at each field when we measured LAI. We calculated  
104 canopy reflectance by dividing plant radiation by sky radiation. We calculated the  
105 normalized difference vegetation index (NDVI) using canopy reflectance in RED  
106 (620-670 nm) and NIR (841–875 nm) (Eq (2)).

$$107 \text{ NDVI} = (\text{reflectance in NIR} - \text{reflectance in RED}) / (\text{reflectance in NIR} + \text{reflectance in RED}) \quad (2)$$

108

#### 109 2.4. SAR images

110 X-band SAR images from the Constellation of Small Satellites for the Mediterranean  
111 Basin Observation COSMO-SkyMed system (ScanSAR Wide Region mode, HH  
112 polarization) were used in this study to acquire high temporal and spatial-resolution  
113 SAR data. COSMO-SkyMed can supply high temporal and spatial-resolution data by  
114 operating 4 satellites on the same orbit. All COSMO-SkyMed images used in this study  
115 were acquired during ascending orbit. The incidence angle for data acquisition was  
116 approximately 45°. Spatial resolution was adjusted to 30 m by multi-look processing  
117 and spatial filtering to reduce speckle noise. The 3 × 3 pixel Lee filter (Lee, 1980) was  
118 applied to the images used in this study. Back scattering coefficients (BSC) of SAR  
119 images is increased as rice plants grow in the paddy fields (Fig.1). Eight SAR images  
120 were obtained from the period between transplanting and heading: on 22 and 30 July, 7,  
121 15, 23 and 31 August and 8 and 16 September. 4 SAR images on 22 July, 7 August, 31  
122 August and 16 September were selected to analyze the relation with LAI and NDVI  
123 measured on 22 - 24 July, 10 - 12 Aug, 30 Aug - 1 Sep and 16 - 18 Sep, respectively.

#### 124 **3. Results and discussion**

125 Back scattering coefficient (BSC) at the investigated fields in SAR images ranged  
126 from -18.3 to -1.57. LAI and NDVI ranged from 0.03 to 3.60 and from -0.24 to 0.81,  
127 respectively. BSC at 28 of 30 fields had a positive correlation with days after  
128 transplanting (DAT), corresponding with rice growth (Fig. 1). However, only 10 of  
129 these results were significant. Observations at the investigated fields indicated that  
130 non-significance was partly caused by deep water or weeds (see Fig. 3).

131 Fig. 2a shows that BSC was significantly correlated with LAI (LAI;  $r = 0.584$ ,  $p <$   
132  $0.001$ ). Although the value was slightly lower than that previously reported (0.75 by  
133 Inoue et al., 2014), the difference might be derived from that between X-band and  
134 C-band. Previous studies also reported that BSC at rice fields showed saturation greater  
135 than 3 in LAI similar to the levels NDVI often suggested (see Fig2c; Capodici et al.,  
136 2013; Inoue et al., 2014). However, BSC in this study did not show such saturation due  
137 to moderate correlation with LAI. Deep water and weeds are generally the factors that  
138 disturbed the relationship between LAI and BSC because BSC is decreased by water  
139 (Martinez and Toan, 2007) and increased by weeds (Liew et al., 1998). In this study,  
140 however, the relationship did not improve even if weedy and DW fields were excluded  
141 from the analysis (Table 1). Fig. 2a and Table 1 shows that BSC and LAI had a closer  
142 correlation at the fields where BSC and DAT had a significant correlation. These results  
143 suggest that the possibility of estimating LAI is dependent on location and that the  
144 observed increase in BSC with DAT is a required condition. Field heterogeneity

145 (Miyaoaka et al., 2013) or orientation of ridge in paddy fields (Yamaguchi et al., 2005)  
146 may cause such locational error. Although further study is necessary, selection of  
147 observation point on the basis of the relation between BSC and DAT in previous seasons  
148 probably improves the estimation accuracy for LAI with BSC.

149 Fig. 2b demonstrates that BSC was also correlated with NDVI ( $r = 0.574$ ,  $p < 0.001$ ).  
150 Although LAI and NDVI displayed a nonlinear relationship (Fig. 2c), no distinct  
151 difference was observed in the relationship between BSC and LAI and that between  
152 BSC and NDVI (Fig. 2a and Fig. 2b). Further studies are necessary to determine what  
153 structural factors in rice canopy affect BSC.

154 The increased rates of BSC against DAT obtained in the fields where BSC and DAT  
155 had a significant correlation were also significantly correlated with LAI growth rate (the  
156 regression line in Fig. 3). However, those fields in which BSC and DAT showed a  
157 non-significant correlation tended to yield lower values of BSC increase rate that  
158 expected from the regression line. This finding suggests that if a significant increase of  
159 BSC against DAT was obtained, the increased rate may represent LAI growth rate.  
160 Hirooka et al. (2015) reported that LAI growth rate was closely associated with soil C  
161 and N levels, which is a major indicator of soil fertility and consequent rice production  
162 in the study area. These facts suggest that soil fertility and rice productivity could be  
163 estimated from BSC even though LAI cannot be directly estimated from BSC.

164 Although LAI ordinarily shows curvilinear growth such as sigmoid, this study  
165 estimated the growth rate by a linear function (Eq. 1) according to Hirooka et al. (2015).  
166 The linear growth indicates that the observation was conducted after exponential growth  
167 and before saturated growth. Low LAI (see Fig. 3a) may help rice to keep linear growth  
168 of LAI before heading. To follow rice growth more precisely, more frequent  
169 measurements are necessary especially just after transplanting and around heading.  
170 Such frequent observation of LAI and BSC might improve the estimation of rice  
171 growth.

172 Rice production in Lao PDR is currently conducted on small and untidy paddy fields  
173 where many trees are left uncut (Kosaka et al., 2006; Miyagawa et al., 2013).  
174 Uncontrollable water levels (drought and deep water) and weeds often constrain rice  
175 production in this area (Inamura et al., 2003; Inthavong et al., 2011). These factors are  
176 unfavorable for evaluating rice growth by SAR images. The dependence on incidence  
177 angle and azimuth angle of the SAR sensor in the relationship between BSC and LAI  
178 should also be analyzed further in order to accurately estimate LAI (Gautier et al., 1998).  
179 Despite the remaining limitations, this study has demonstrated the capacity of SAR to  
180 evaluate rice production in developing countries. Combining an area map of planted rice

181 as well as planting dates both of which are obtained from SAR images (Miyaoaka et al.,  
182 2013; Maki et al., 2015) may help a more accurate evaluation of rice productivity.

183

#### 184 **Acknowledgements**

185 This research was supported by the environmental research & technology development fund  
186 (E-1104: Development and Practice of Advanced Basin Model in Asia: Toward Adaptation of  
187 climate Changes (FY2011–FY2013), Ministry of the Environment, Japan), by the green  
188 network of excellence, Ministry of Education, Culture, Sport, Science and Technology, Japan  
189 and by Japan Society for the Promotion of Science.

190

#### 191 **References**

- 192 Bamler, R., 2000. Principles of synthetic aperture radar. *Surveys in Geophysics* 21,  
193 147-157.
- 194 Bell, R.W., and Seng, V., 2003. Rainfed lowland rice-growing soils of Cambodia, Laos,  
195 and North-east Thailand. *CARDI International Conference on Research on Water in  
196 Agricultural Production in Asia for the 21st Century*, 25 – 28 November, Phnom Penh,  
197 Cambodia, 161-173.
- 198 Capodici, F., D’Urso, G., Maltese, A., 2013. Investigating the relationship between  
199 X-band SAR data from COSMO-SkyMed satellite and NDVI for LAI detection.  
200 *Remote Sensing* 5, 1389–1404.
- 201 Chakraborty, M., Manjunath, K. R., Panigrahy, S., Kundu, N., Parihar, J. S., 2005. Rice  
202 crop parameter retrieval using multi-temporal, multi-incidence angle RADARSAT  
203 SAR data. *ISPRS Journal of Photogrammetry and Remote Sensing* 59, 310–322.
- 204 Fukai, S., Inthapanya, P., Blamey, F.P.C., Khonthosuvon, S., 1999. Genotypic variation  
205 in rice grown in low fertile soils and drought-prone, rainfed lowland environments.  
206 *Field Crops Research* 64, 121–130.
- 207 Gauthier, Y., Bernier, M., Fortin, J. P., 1998. Aspect and incidence angle sensitivity in  
208 ERS-1 SAR data. *International Journal of Remote Sensing* 19, 2001–2006.
- 209 Hirooka, Y., Homma, K., Maki, M., Sekiguchi, K., Shiraiwa, T., Yoshida, K., 2015.  
210 Evaluation of the dynamics of the leaf area index (LAI) of rice in farmer’s fields in  
211 Vientiane Province, Lao PDR. *Journal of Agricultural Meteorology* (in press).
- 212 Inamura, T., Miyagawa, S., Singvilay, O., Sipaseauth, N., Kono, Y., 2003. Competition  
213 between weeds and wet season transplanted paddy rice for nitrogen use, growth and  
214 yield in the central and northern regions of Laos. *Weed Biology and Management* 3,  
215 213-221.
- 216 Inoue, Y., Sakaiya, E., Wang, C., 2014. Capability of C-band backscattering coefficients

217 from high-resolution satellite SAR sensors to assess biophysical variables in paddy  
218 rice. *Remote Sensing on Environment* 140, 257-266.

219 Inthavong, T., Tsubo, M., Fukai, S., 2011. A water balance model for characterization of  
220 length of growing period and water stress development for rainfed lowland rice. *Field*  
221 *Crops Research* 121, 291–301.

222 Kosaka, Y., Takeda, S., Prixar, S., Sithirajvongsa, S., Xaydala, K., 2006. Species  
223 composition, distribution and management of trees in rice paddy fields in central Lao,  
224 PDR. *Agroforestry Systems* 67, 1 – 17.

225 Lee, J. S., 1980. Digital image enhancement and noise filtering by use of local statistics.  
226 *IEEE Transactions on Pattern Analysis and Machine Intelligence* 2, 165-168.

227 Liew, S.C., Kam, S.P., Tuong, T.P., Chen, P., Minh, V.Q., Lim, H. 1998. Application of  
228 multitemporal ERS-2 synthetic aperture radar in delineating rice cropping systems in  
229 the Mekong River Delta, Vietnam. *Geoscience and Remote Sensing*, 36, 1412-1420.

230 Maclean, J.L., Dawe, D.C., Hardy, B., Hettel, G.L., 2002. Rice almanac: Source book  
231 for the most important economic activity on earth. (Philippines): International Rice  
232 Research Institute, Los Banos, 1-253.

233 Maki, M., Homma, K., Hirooka, Y., Oki, K. 2015. Development and practice of  
234 advanced basin model in Asia -Estimation of rice yield by assimilating remote sensing  
235 data into crop growth model (SIMRIW-RS). *Journal of Agricultural Meteorology* (in  
236 press).

237 Martinez J.M., Le Toan T. 2007 Mapping of flood dynamics and spatial distribution of  
238 vegetation in the Amazon floodplain using multitemporal SAR data. *Remote Sensing*  
239 *of Environment* 108, 209–223.

240 Miyagawa, S., Seko, M., Harada, M., Sivilay, S., 2013. Yields from Rice Plants  
241 Cultivated under Tree Canopies in Rainfed Paddy Fields on the Central Plain of Laos.  
242 *Plant Production science* 16, 325-334.

243 Miyaoka, K., Maki, M., Susaki, J., Homma, K., Noda, K., Oki, K., 2013. Rice-planted  
244 area mapping using small sets of multi-remporal SAR data. *IEEE Geoscience and*  
245 *Remote Sensing Letters* 10, 1507-1511.

246 Schiller, J.M. 2006. Rice in Laos. International Rice Research Institute, Metro Manila,  
247 1-457.

248 Moran M.S, Hymer, D.C., Qi, J.G., Kerr, Y., 2002. Comparison of ERS-2 SAR and  
249 Landsat TM imagery for monitoring agricultural crop and soil conditions, *Remote Sens.*  
250 *Environ* 79, 243 -252.

251 Yamaguchi, Y., Moriyama, T., Ishido, M., Yamada, H. 2005. Four-component scattering  
252 model for polarimetric SAR image decomposition. *Geoscience and Remote Sensing*, 43,

253 1699-1706.

254

255

256



257 Figure captions

258

259 Fig.1 The map of Google earth (left) and synthetic aperture radar (SAR) images (center  
260 and right) for a part of the research area. Back scattering coefficient (BSC) is  
261 gray-scaled in the SAR images. The increase of BSC (gray in 22 July to white in 16  
262 September) corresponded to the rice growth in paddy fields.

263

264 Fig. 2 Changes in the back scattering coefficient (BSC) with days after transplanting  
265 (DAT) at the two fields where BSC and DAT had a significant correlation. The slope of  
266 the regression line was defined as rate of BSC increase.

267

268 Fig. 3 Relationship between (a) back scattering coefficient (BSC) and leaf area index  
269 (LAI), (b) BSC and normalized difference vegetation index (NDVI), (c) LAI and NDVI.  
270 S: the field where BSC and DAT had a significant correlation. N: the field where BSC  
271 and DAT had a non-significant correlation. DW: the field that had more than 30 cm  
272 depth of standing water. Weed: the field covered by more than 20% weeds at the  
273 maximum.

274

275 Fig. 4 Relationship between leaf area index (LAI) growth rate ( $\text{m}^2 \text{m}^{-2} \text{day}^{-1}$ ) and back  
276 scattering coefficient (BSC) increase rate ( $\text{day}^{-1}$ ). The line was regressed by the field  
277 where BSC and DAT had a significant correlation (S). The symbols are the same in Fig.  
278 3; The fields which were classified into DW or Weed at least one time in Fig. 3 were  
279 defined as DW or Weed fields, respectively.

280

281 Table 1 Correlation coefficients of back scattering coefficient (BSC) with leaf area  
282 index (LAI and normalized difference vegetation index (NDVI). Except DW: DW fields  
283 were excluded from the correlation; Except Weed: Weed fields were excluded from the  
284 correlation; Except N: the fields where BSC and DAT had a non-significant correlation  
285 were excluded from the correlation; see Fig. 3.

286

1 Table 1 Correlation coefficients of back scattering coefficient (BSC) with leaf area  
2 index (LAI) and normalized difference vegetation index (NDVI). Except DW: DW  
3 fields were excluded from the correlation; Except Weed: Weed fields were excluded  
4 from the correlation; Except N: the fields where BSC and DAT had a non-significant  
5 correlation were excluded from the correlation; see Fig. 3.

6

7

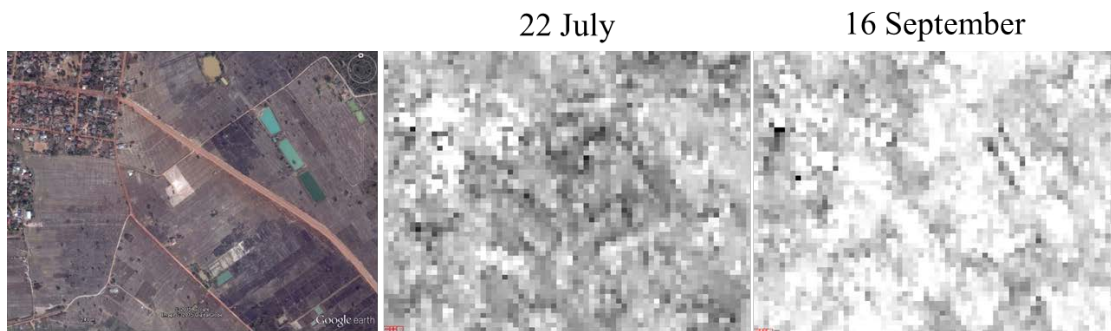
	LAI	NDVI
All	0.584	0.574
Except DW	0.551	0.509
Except Weeds	0.603	0.585
Except N	0.766	0.593

8

9

10

11



13

14 Fig.1 The map of Google earth (left) and synthetic aperture radar (SAR) images  
15 (center and right) for a part of the research area. Back scattering coefficient (BSC) is  
16 gray-scaled in the SAR images. The increase of BSC (gray in 22 July to white in 16  
17 September) corresponded to the rice growth in paddy fields.

18

19

20

21

22

23

24

25

26

27

28

29

30

31

32

33

34

35

36

37

38

39

40  
41  
42  
43  
44  
45  
46  
47  
48  
49  
50  
51  
52  
53  
54  
55  
56  
57  
58  
59  
60  
61  
62  
63  
64  
65  
66  
67  
68  
69  
70  
71  
72  
73  
74  
75

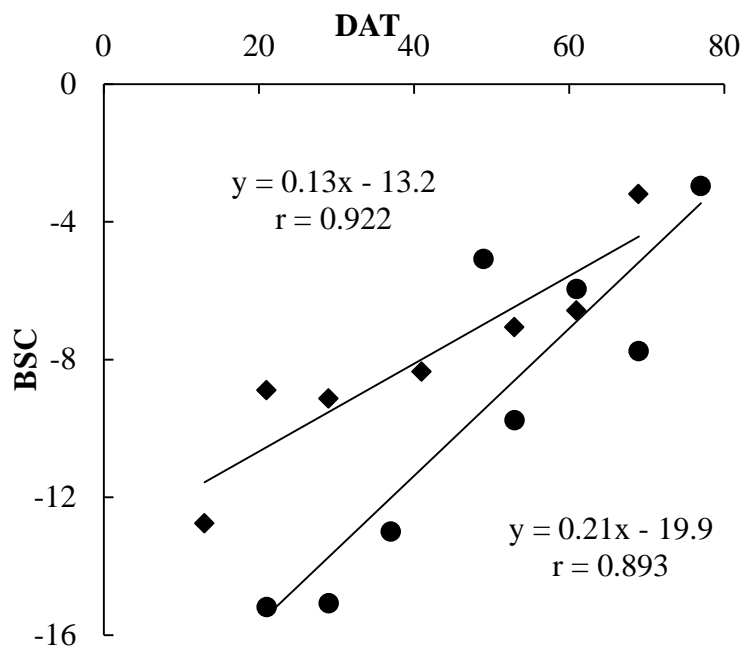
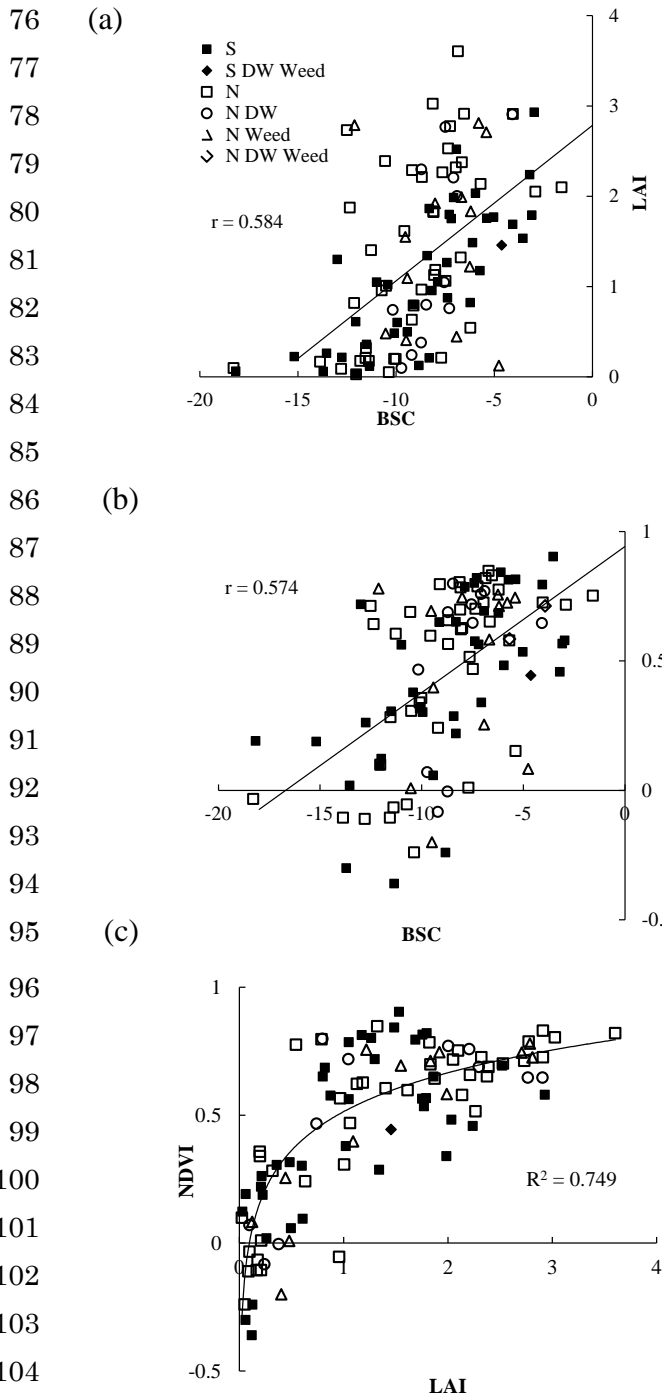


Fig. 2 Changes in the back scattering coefficient (BSC) with days after transplanting (DAT) at the two fields where BSC and DAT had a significant correlation. The slope of the regression line was defined as rate of BSC increase.



106 Fig. 3 Relationship between (a) back scattering coefficient (BSC) and leaf area index  
 107 (LAI), (b) BSC and normalized difference vegetation index (NDVI), (c) LAI and NDVI.  
 108 S: the field where BSC and DAT had a significant correlation. N: the field where BSC  
 109 and DAT had a non-significant correlation. DW: the field that had more than 30 cm  
 110 depth of standing water. Weed: the field covered by more than 20% weeds at the  
 111 maximum.

112  
113  
114  
115  
116  
117  
118  
119  
120  
121  
122  
123  
124  
125  
126  
127  
128  
129  
130  
131  
132  
133  
134  
135  
136  
137  
138  
139  
140  
141  
142  
143  
144  
145  
146  
147

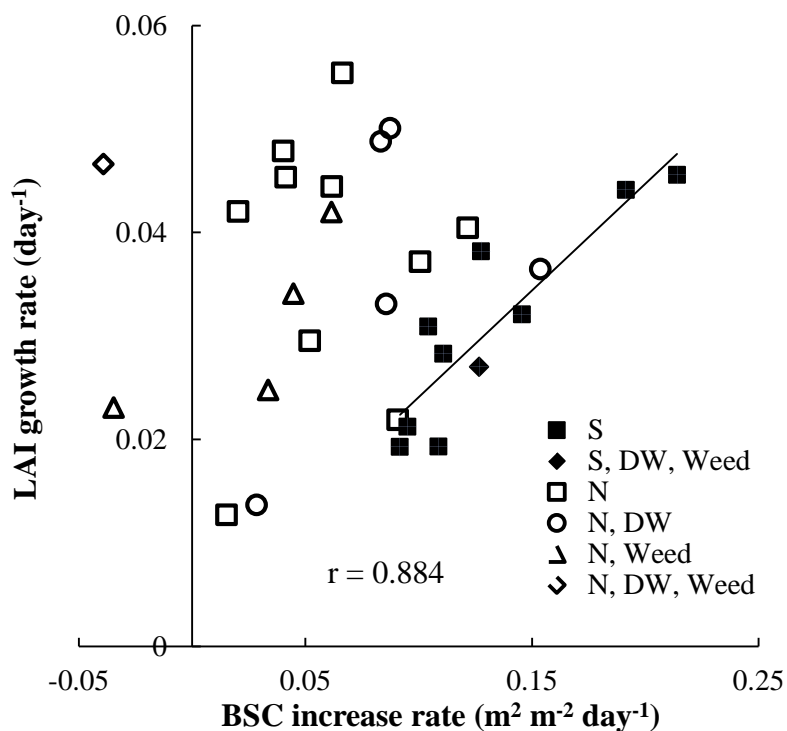


Fig. 4 Relationship between leaf area index (LAI) growth rate (m<sup>2</sup> m<sup>-2</sup> day<sup>-1</sup>) and back scattering coefficient (BSC) increase rate (day<sup>-1</sup>). The line was regressed by the field where BSC and DAT had a significant correlation (S). The symbols are the same in Fig. 3; The fields which were classified into DW or Weed at least one time in Fig. 3 were defined as DW or Weed fields, respectively.